

Theoretical Investigation on Structures, Densities, Detonation Properties, and the Pyrolysis Mechanism of the Derivatives of HNS

Wang Gui-xiang,[†] Shi Chun-hong,[‡] Gong Xue-dong,[†] and Xiao He-ming^{*†}

Computation Institute for Molecules and Materials, Department of Chemistry, Nanjing University of Science and Technology, Nanjing 210094, China, and Shaanxi Applied Physics and Chemistry Research Institute, Xi'an 710061, China

Received: June 4, 2008; Revised Manuscript Received: December 11, 2008

The derivatives of 2,2',4,4',6,6'-hexanitrostilbene (HNS) are optimized to obtain their molecular geometries and electronic structures at the DFT-B3LYP/6-31G* level. Detonation properties are evaluated using the modified Kamlet–Jacobs equations based on the calculated densities and heats of formation. It is found that there are good linear relationships between the density, detonation velocity, detonation pressure, and number of nitro, amino, and hydroxy groups. The thermal stability and pyrolysis mechanism of the title compounds are investigated by calculating the bond dissociation energies at the unrestricted B3LYP/6-31G* level. For the nitro and amino derivatives of HNS, the C–NO₂ bond is a trigger bond during the thermolysis initiation process, while for hydroxy derivatives, it is started from the isomerization reaction of the hydrogen transfer in the O–H bond. According to the quantitative standard of energetics and stability, as high-energy density compounds, 2,2',3,3',4,4',5,6,6'-nonanitrostilbene and 2,2',3,3',4,4',5,5',6,6'-decanitrostilbene essentially satisfy this requirement. In addition, we have discussed the effect of the nitro, amino, and hydroxy groups on the structure and properties.

1. Introduction

2,2',4,4',6,6'-Hexanitrostilbene (HNS), since it was synthesized, has been widely used as a typical secondary explosive in thermally stable charges or perforators, including secondary fillings of detonators for deep boreholes (high temperatures and pressures in exploitation of oil and nature gas), because of its structural stability, higher energy, and good detonation properties. Therefore, it has been receiving considerable attention and a lot of investigations.^{1–6} However, previous studies mainly focused on thermal decomposition and discussed new synthetic techniques using experimental methods, but theoretical studies are few. To date, only the structures and stability of the amino derivatives of HNS have been theoretically studied using a semiempirical molecular orbital (MO) method, and at the same time, the molecular design was simply considered.⁷ Because studies on structure–performance relationships are the foundation of molecular design, in this paper, a series of the nitro, amino, and hydroxy derivatives of HNS (see Figure 1 for the structural diagrams of these compounds) are fully optimized at the DFT-B3LYP/6-31G* level to obtain the molecular geometries, electronic structures, molecular volumes (*V*), theoretical densities (ρ), detonation velocities (*D*), and detonation pressures (*P*), as well as bond dissociation energies (BDEs) of the main bonds. The pyrolysis mechanism, thermal stability, and sensitivity are studied.

In the past decade, our group has carried out a series of investigations on the “molecular design” of high-energy density compounds (HEDCs) for many typical categories of energetic compounds.^{8–17} On the basis of the conventional opinion¹⁸ and our study, quantitative criteria considering both energy (including ρ , *D*, and *P*) and stability (BDE of the trigger bond) requirements, i.e., $\rho \approx 1.9 \text{ g/cm}^3$, *D* $\approx 9.0 \text{ km/s}$, *P* $\approx 40.0 \text{ GPa}$,

and BDE $\approx 80\text{--}120 \text{ kJ/mol}$, are employed to filtrate and recommend potential HEDCs from the title compounds.¹⁷

The systematic theoretical studies on the structures and properties provide an abundance of information and lay a good foundation for the molecular design of the energetic and secondary explosives.

2. Computational Methods

Many studies^{8,10,19} have shown that the DFT-B3LYP method^{20,21} in combination with the 6-31G*²² basis set is able to give accurate energies, molecular structures, and a series of properties. In this paper, the derivatives of HNS are fully optimized to obtain their molecular geometries and electronic structures at this level with the *Gaussian03* program package.²³

The detonation velocity and pressure are the most important parameters for evaluating the detonation characteristics of energetic materials. For the explosives with CHNO elements, these parameters can be calculated using the Kamlet–Jacobs (K–J) equations^{24,25}

$$D = (1.011 + 1.312\rho_0)(NM^{0.5}Q^{0.5})^{0.5} \quad (1)$$

$$P = 1.558\rho_0^2 NM^{0.5} Q^{0.5} \quad (2)$$

where *P* is the detonation pressure (GPa), *D* is the detonation velocity (km/s), ρ_0 is the packed density (g/cm³), *N* is the moles of gas produced per gram of explosives, \bar{M} is the average molar weight of detonation products, and *Q* is the chemical energy of detonation (kJ/g). *N*, \bar{M} , and *Q* are decided according to the largest exothermic principle; i.e., for the explosives with CHNO elements, all of the N atom converts into N₂, the O atom forms H₂O with the H atom first, and the remainder forms CO₂ with the C atom. The remainder of the C atom will exist in the solid state if the O atom does not satisfy full oxidation of the C atom. The remainder of the O atom will exist in O₂ if the O atom is superfluous. Table

* Corresponding author. Telephone and Fax: +86-25-84303919. E-mail: xiao@mail.njust.edu.cn.

[†] Nanjing University of Science and Technology.

[‡] Shaanxi Applied Physics and Chemistry Research Institute.

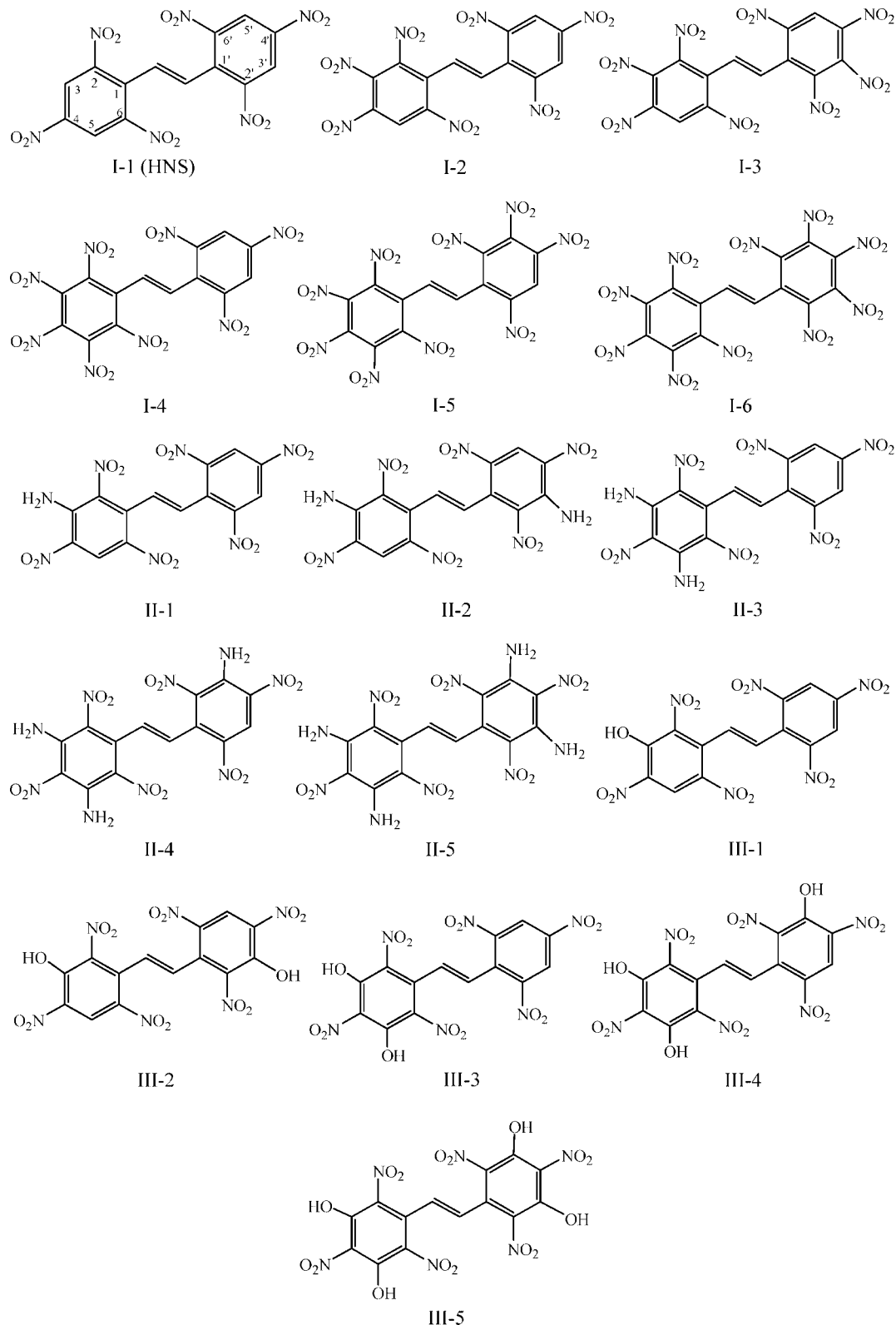


Figure 1. Illustration of the molecular structures of the derivatives of HNS (H atoms are omitted for clarity).

I presents the methods for calculating the N , \bar{M} , and Q parameters of the CaHbOcNd explosive.

Obviously, for known explosives, their Q and ρ_0 can be measured experimentally; thus, their D and P can be calculated according to eqs 1 and 2. However, for those unsynthesized explosives and hypothetical compounds, their Q and ρ_0 cannot be evaluated from experimental measures. Therefore, in the molecular

design of HEDC, in order to predict the detonation properties, we recommend the modified K–J equations based on the calculation results of quantum chemistry.^{8–17}

In detail, the loading density of the explosives ρ_0 can be replaced by the crystal theoretical density (ρ_{cry}), while the chemical energy of the detonation reaction Q can be calculated as the difference between the heats of formation

TABLE 1: Methods for Calculating the N , \bar{M} , and Q Parameters of the CaHbOcNd Explosive^a

parameter	stoichiometric ratio		
	$c \geq 2a + b/2$	$2a + b/2 > c \geq b/2$	$b/2 > c$
N	$(b + 2c + 2d)/4M$	$(b + 2c + 2d)/4M$	$(b + d)/2M$
\bar{M}	$4M/(b + 2c + 2d)$	$(56d + 88c - 8b)/(b + 2c + 2d)$	$(2b + 28d + 32c)/(b + d)$
$Q \times 10^{-3}$	$(28.9b + 94.05a + 0.239\Delta H_f^\circ)/M$	$[28.9b + 94.05(c/2 - b/4) + 0.239\Delta H_f^\circ]/M$	$(57.8c + 0.239\Delta H_f^\circ)/M$

^a a , b , c , and d stand for the number of C, H, O, and N atoms in the compound, respectively; M in the formula is the molecular weight of the title compounds (in g/mol); ΔH_f° is the standard heat of formation of the studied compound (in kJ/mol).

TABLE 2: Predicted Densities and Detonation Properties of the Title Compounds^a

no.	Chemical name	OB ₁₀₀	Q	HOF	V	ρ	D	P
I-1	2,2',4,4',6,6'-hexanitrostilbene	-2.22	1428.4	194.52	247.57	1.82 (1.79) ³⁵	7.59	25.75
I-2	2,2',3,4,4',6,6'-heptanitrostilbene	-1.01	1503.1	245.67	266.78	1.86	7.98	28.80
I-3	2,2',3,3',4,4',6,6'-octanitrostilbene	0.00	1568.6	305.63	282.99	1.91	8.36	32.10
I-4	2,2',3,4,4',5,6,6'-octanitrostilbene	0.00	1568.5	305.39	283.01	1.91	8.36	32.10
I-5	2,2',3,3',4,4',5,6,6'-nonanitrostilbene	0.85	1624.0	365.43	299.76	1.95	8.68	35.00
I-6	2,2',3,3',4,4',5,5',6,6'-decanitrostilbene	1.90	1659.3	438.23	316.35	1.99	8.90	37.21
II-1	3-amino-2,2',4,4',6,6'-hexanitrostilbene	-2.37	1379.4	165.01	258.19	1.80	7.54	25.23
II-2	3,3'-diamino-2,2',4,4',6,6'-hexanitrostilbene	-2.50	1340.7	151.41	263.11	1.82	7.61	25.87
II-3	3,5-diamino-2,2',4,4',6,6'-hexanitrostilbene	-2.50	1334.7	139.29	264.18	1.82	7.60	25.82
II-4	3,3',5-triamino-2,2',4,4',6,6'-hexanitrostilbene	-2.63	1298.6	125.75	268.76	1.84	7.67	26.44
II-5	3,3',5,5'-tetramino-2,2',4,4',6,6'-hexanitrostilbene	-2.74	1258.8	99.96	279.62	1.82	7.61	25.85
III-1	3-hydroxy-2,2',4,4',6,6'-hexanitrostilbene	-1.72	1375.2	-11.79	251.02	1.86	7.71	26.92
III-2	3,5-dihydroxy-2,2',4,4',6,6'-hexanitrostilbene	-1.24	1329.2	-209.28	257.45	1.87	7.75	27.2
III-3	3,3'-dihydroxy-2,2',4,4',6,6'-hexanitrostilbene	-1.24	1327.9	-211.85	257.87	1.87	7.75	27.23
III-4	3,3',5-trihydroxy-2,2',4,4',6,6'-hexanitrostilbene	-0.80	1286.2	-406.66	263.86	1.89	7.81	27.84
III-5	3,3',5,5'-tetrahydroxy-2,2',4,4',6,6'-hexanitrostilbene	-0.39	1244.0	-608.08	267.46	1.92	7.89	28.69

^a Units: HOF/(kJ/mol), Q /(J/g), V /(cm³/mol), ρ /(g/cm³), D /(km/s), and P /Gpa. The experimental value appears in parentheses.

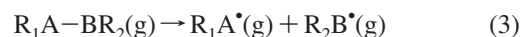
(HOFs) of products and those of reactants (Q_{cal}). However, from the K–J equations, it is found that Q has much less effect than ρ on D and P . Therefore, Q and HOF estimated using the semiempirical MO PM3²⁶ method are precise enough to substitute the experimental data, as has been proven in previous studies.²⁷ On the basis of ρ and Q , the corresponding D and P can be evaluated. In practice, ρ_0 can only approximate to but not arrive at ρ ; thus, D and P obtained from ρ can be seen as their upper limit (maximum values).

As is known to all, accurate prediction of the crystal density is very difficult. A “group or volume additivity” method,^{28,29} although simple and rapid, cannot give reliable results because of its inherent drawbacks, while the “crystal packing” method,^{30,31} which is more reliable, has its limitation in routine calculation because of its extensive requirement of computational resources. Recently, an efficient and convenient way has been worked out to predict the crystalline densities of energetic materials containing C, H, N, and O elements.³² Studies have indicated that,³² when the average molar volume V estimated by the Monte Carlo method based on 0.001 electrons/bohr³ density space at the B3LYP/6-31G** or 6-31G* level is used, the theoretical molecular density ρ_{mol} ($\rho_{mol} = M/V$, where M is the molecular weight) is very close to the experimental crystal density ρ_{cry} . It is worth noting that the average volume used here should be the statistical average of at least 100 volume calculations.

In a word, the modified K–J equation has been endowed with the new connotation, and its application range has been extended. Also, on the basis of quantum chemistry, it has been used to calculate D and P to quantitatively evaluate HEDC in molecular design. The modified method has resulted in satisfactory results.^{8–17}

To measure the strength of the bonds and relative stabilities of the title compounds, the BDEs of various bonds in the molecule are calculated. BDE is the required energy for homolysis of a bond and is commonly denoted by the difference

between the total energies of the product and reactant after zero-point-energy correction. The expressions for homolysis of a A–B bond (eq 3) and for calculation of its BDE (eq 4) are shown as follows:³³



$$BDE_{R_1A-BR_2} = [E_{R_1A^\bullet} + E_{R_2B^\bullet}] - E_{R_1A-BR_2} \quad (4)$$

where R_1A-BR_2 stands for the neutral molecules and R_1A^\bullet and R_2B^\bullet stand for the corresponding product radicals after the bond dissociation; $BDE_{R_1A-BR_2}$ is the BDE of the bond R_1A-BR_2 ; $E_{R_1A-BR_2}$, $E_{R_1A^\bullet}$, and $E_{R_2B^\bullet}$ are the zero-point-corrected total energies of the parent compound and the corresponding radicals, respectively.

All of the calculations considered here were performed on a Pentium IV personal computer using the default convergence criteria given in the programs.

3. Results and Discussion

3.1. Densities and Energies. Table 2 collects V , ρ , D , and P of the title compounds. The oxygen balances (OB₁₀₀), calculated HOFs, and Q 's are also listed in this table.

The oxygen balances (OB₁₀₀) are calculated using the formula (5), which can be used to roughly predict the impact sensitivities of the explosives.³⁴

$$OB_{100} = \frac{100(2n_O - n_H - 2n_C - 2n_{COO})}{M} \quad (5)$$

where n_O , n_H , and n_C represent the numbers of O, H, and C atoms, respectively; n_{COO} is the number of COO–, and here $n_{COO} = 0$ for the derivatives of HNS; M is the molecular weight.

From Table 2, we see that the calculated density (1.82 g/cm³) agrees well with the available experimental value (1.79 g/cm³), which indicates that the theoretical density calculated at the

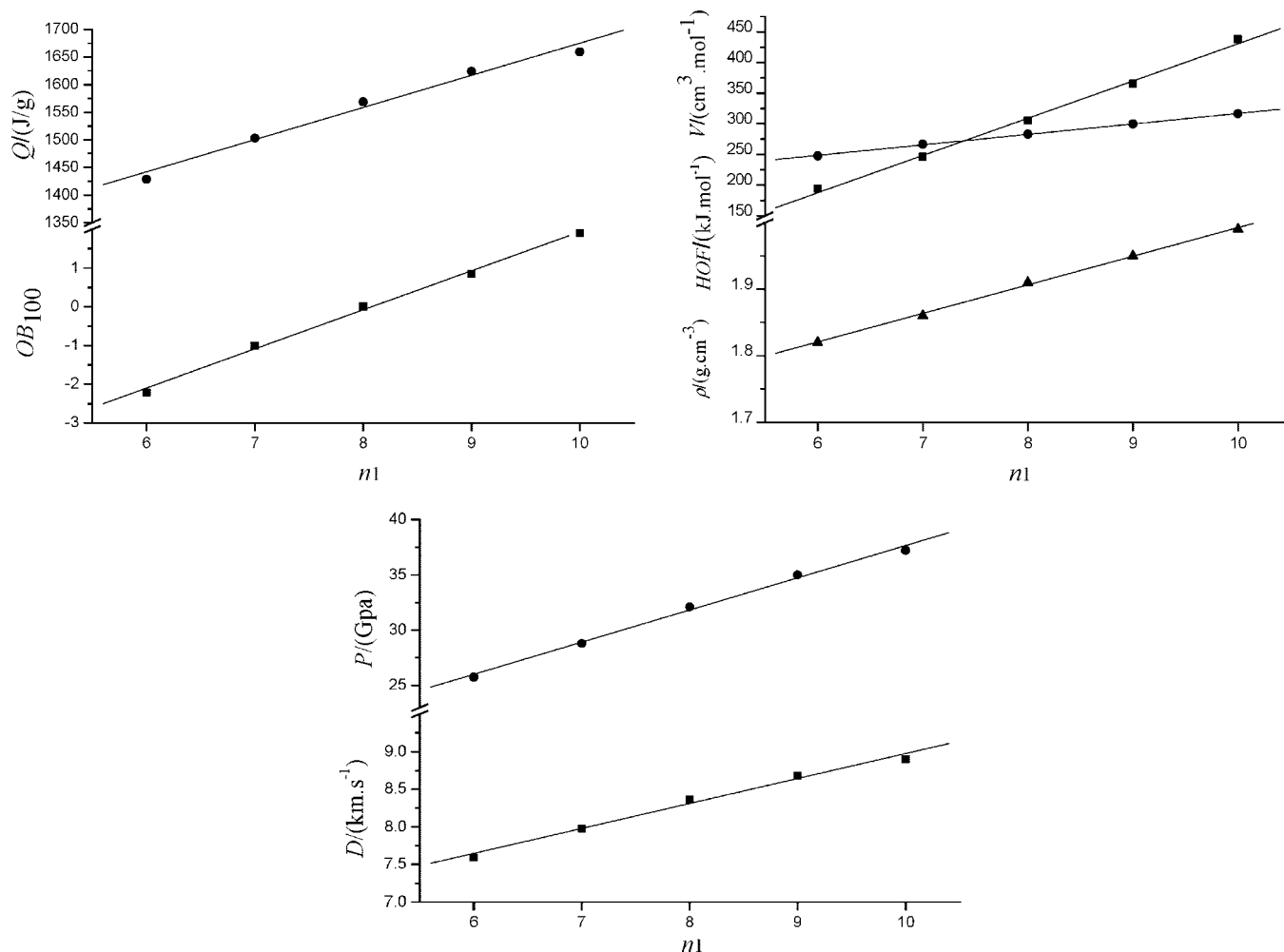


Figure 2. Correlations between OB_{100} , ΔH_f , Q , V , ρ , D , P , and the number of nitro groups (n_1) for the nitro derivatives of HNS.

B3LYP/6-31G* level is truly close to the crystal density. This may reflect that, according to the modified K–J equation, our predictions of the detonation properties for the title compounds will be reliable. In fact, many previous studies have shown the reliability of the calculation method.¹⁷

It can also be seen from Table 2 that the energy and density of HNS are linearly improved when it is substituted with $-\text{NO}_2$ and $-\text{OH}$ groups. However, substitution of a $-\text{NH}_2$ group has little effect on the density of HNS, which shows that the introduction of an amino group cannot improve the detonation properties of HNS.

Taking the nitro derivatives of HNS (I-1–I-6) as an example, Figure 2 presents the relationships between OB_{100} , ΔH_f , Q , V , ρ , D , P , and the number of nitro groups (n_1), which all exist as linear relationships, obviously showing good group additivity. The correlation equations are $OB_{100} = -8.16 + 1.01n_1$, $HOF = -176.60 + 60.72n_1$, $Q = 1092.49 + 58.27n_1$, $V = 146.31 + 17.05n_1$, $\rho = 1.56 + 0.04n_1$, $D = 5.66 + 0.33n_1$, and $P = 8.53 + 12.91n_1$, respectively, and the corresponding correlation coefficients are 0.9980, 0.9979, 0.9899, 0.9995, 0.9988, 0.9933, and 0.9971, respectively. This strongly supports the claim that introducing more nitro substituents (moderately increasing the oxygen balance) into an energetic molecule usually helps to increase its detonation performance.²⁵

The detonation performances of the nitro derivatives of HNS are close to those of the important explosive 1,3,5-trinitro-1,3,5-triazinane (RDX; $\rho = 1.81 \text{ g/cm}^3$, $D = 8.75 \text{ km/s}$, and $P = 34.70 \text{ GPa}$) when the number of nitro groups (n_1) is equal to or

more than 8. When n_1 is 10, e.g., I-6, its detonation performances ($\rho = 1.99 \text{ g/cm}^3$, $D = 8.90 \text{ km/s}$, and $P = 37.21 \text{ GPa}$) are the best and almost close to those of the more important explosive 1,3,5,7-tetranitro-1,3,5,7-tetrazocane (HMX; $\rho = 1.90 \text{ g/cm}^3$, $D = 9.10 \text{ km/s}$, and $P = 39.00 \text{ GPa}$), which indicates that I-6 is a possible potential HEDC.

For the amino derivatives of HNS (II-1–II-5), OB_{100} , HOF, Q , and V all linearly decrease or increase with the number of amino groups (n_2), but the variations of ρ , D , and P are very little (see Figure 3), which again indicates that substitution of a $-\text{NH}_2$ group has little effect on the density and detonation properties and that possibly increases the stability of HNS. However, for the amino derivatives of HNS, the variation of ρ does not correlate with the number of amino groups because of the presence of intermolecular and intramolecular hydrogen bonds; therefore, D and P do not linearly increase with the number of amino groups. Here, only the linear relationships between OB_{100} , ΔH_f , Q , V , and the number of amino groups (n_2) are presented as follows:

$$OB_{100} = -2.23 - 0.13n_2, \quad R = -0.9984, \quad SD = 0.0116$$

$$HOF = 191.67 - 22.84n_2, \quad R = -0.9902, \quad SD = 5.0957$$

$$Q = 1424.10 - 42.00n_2, \quad R = -0.9982, \quad SD = 3.9636$$

$$V = 248.64 + 7.47n_2, \quad R = 0.9890, \quad SD = 1.7682$$

For the hydroxy derivatives of HNS (III-1–III-5), OB_{100} , V , ρ , D , and P , except HOF and Q , which linearly decrease,

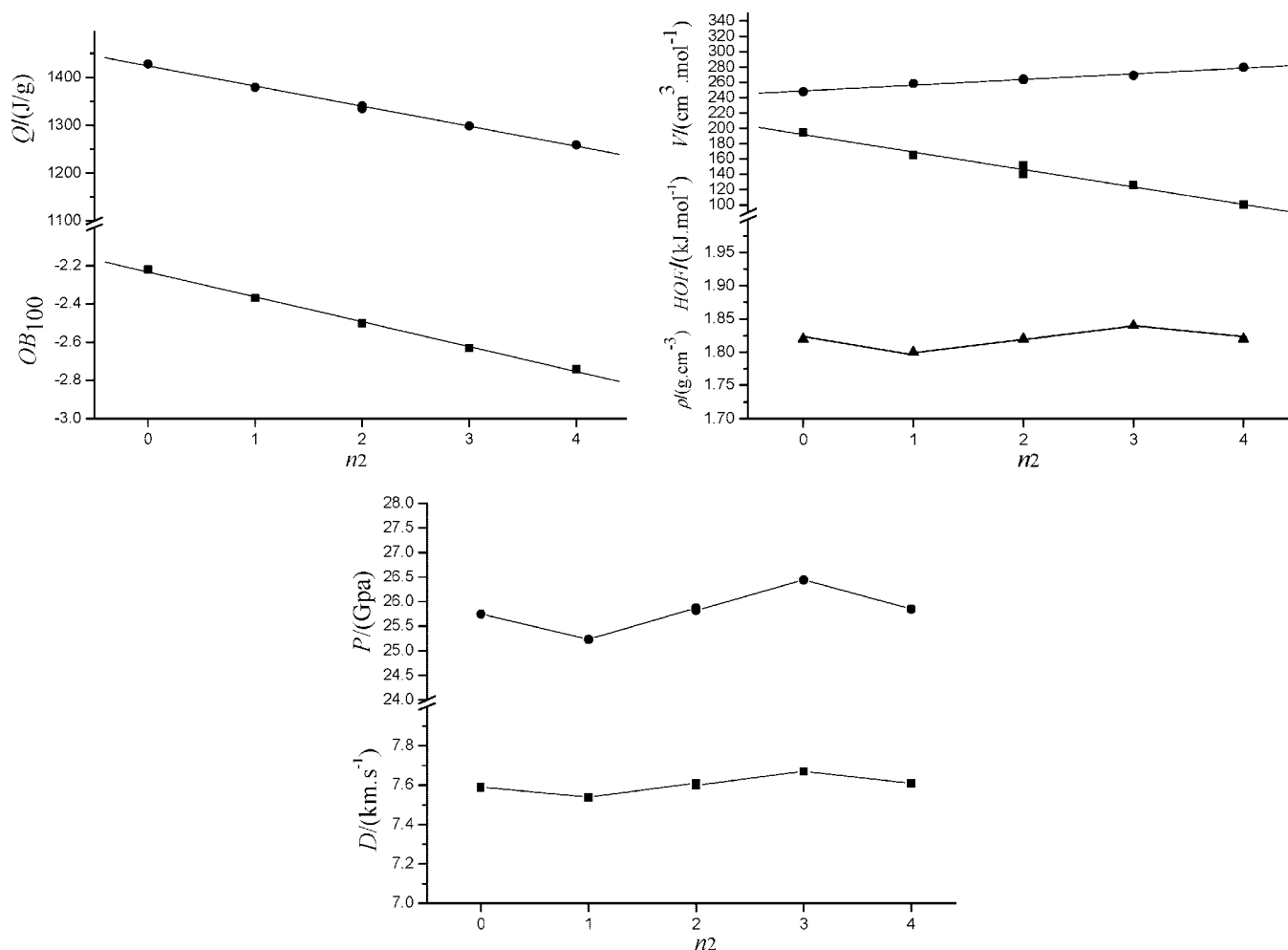


Figure 3. Correlations between OB_{100} , ΔH_f , Q , V , ρ , D , P , and the number of amino groups (n_2) for the amino derivatives of HNS.

increase with the number of hydroxy groups (n_3 ; see Figure 4). Their linear relationships are $OB_{100} = -2.18 + 0.46 n_3$ ($R = 0.9989$), $HOF = 191.16 - 200.01n_3$ ($R = 1.0000$), $Q = 1423.38 - 45.78n_3$ ($R = -0.9984$), $V = 247.01 + 5.26n_3$ ($R = 0.9938$), $\rho = 1.83 + 0.02n_3$ ($R = 0.9822$), $D = 7.61 + 0.07n_3$ ($R = 0.9860$), and $P = 25.92 + 0.68n_3$ ($R = 0.9839$).

On the whole, the density and detonation performances of the hydroxy derivatives of HNS are improved and are between those of the nitro and amino derivatives. Therefore, it is worth studying their stability.

3.2. Pyrolysis Mechanism, Stability, and Identification of Sensitivity. **3.2.1. Bond Overlap Populations.** Bond overlap populations reflect the electron accumulations in the bonding region, and they can provide us with detailed information about the chemical bond. As a whole, the fewer Mulliken bond populations that a bond has, the easier the bond breaks. Though Mulliken population analysis³⁶ suffers from some shortcomings, such as the basis set dependence, results derived from the Mulliken population analysis at the same calculation conditions are still meaningful for comparing trends in the electron distribution for homologous compounds, as was done here. The bond orders obtained from the Mulliken population analysis for the title compounds at the B3LYP/6-31G* level are listed in Table 3.

Upon inspection of the data in Table 3, it can be found that the overlap population of the C–NO₂ bond (M_{C-NO_2}) is the least in each molecule of the title compounds. However, for the hydroxy derivatives of HNS (III-1–III-5), the overlap population

of the O–H bond (M_{O-H}) close to M_{C-NO_2} is also relatively smaller than other bonds, which indicates that the C–NO₂ and O–H bonds may be the trigger bonds during thermolysis initiation process.

Meanwhile, for the nitro derivatives of HNS (I-1–I-6), on the whole, with the number of nitro groups increasing, M_{C-NO_2} decreases as expected. This suggests that the stability decreases and that their sensitivities increase accordingly, which confirms that the nitro group has an effect on the activity. For example, the order of the stability from I-1 to I-6 is I-6 \approx I-5 \approx I-4 < I-3 < I-2 < I-1. For the amino derivatives of HNS (II-1–II-5), with the number of amino groups increasing, M_{C-NO_2} increases, indicating that their stability increases and sensitivity decreases, which similarly confirms that the amino group has an insensitizing effect. For instance, the order of the stability for II-1–II-5 compounds is II-1 < II-2 (0.1474) \approx II-3 (0.1471) < II-4 < II-5. From Table 3, it also can be seen that, for the hydroxy derivatives of HNS (III-1–III-5), with the number of hydroxy groups increasing, the variational trend of M_{C-NO_2} is in accordance with that of M_{O-H} and is smaller than that of M_{C-NO_2} of HNS (0.1468). This indicates that the hydroxy group has a sensitizing effect. However, it is noticeable that M_{C-NO_2} of III-1 (0.1306) is almost equal to those of III-2 (0.1303) and III-4 (0.1304) and that of III-3 (0.1422) is almost equal to that of III-5 (0.1420), which infers that there is not much doubt about the number of the hydroxy groups having an influence on the stability of the molecules, but the position of the hydroxy group is more important. Therefore, the four-substituted HNS is

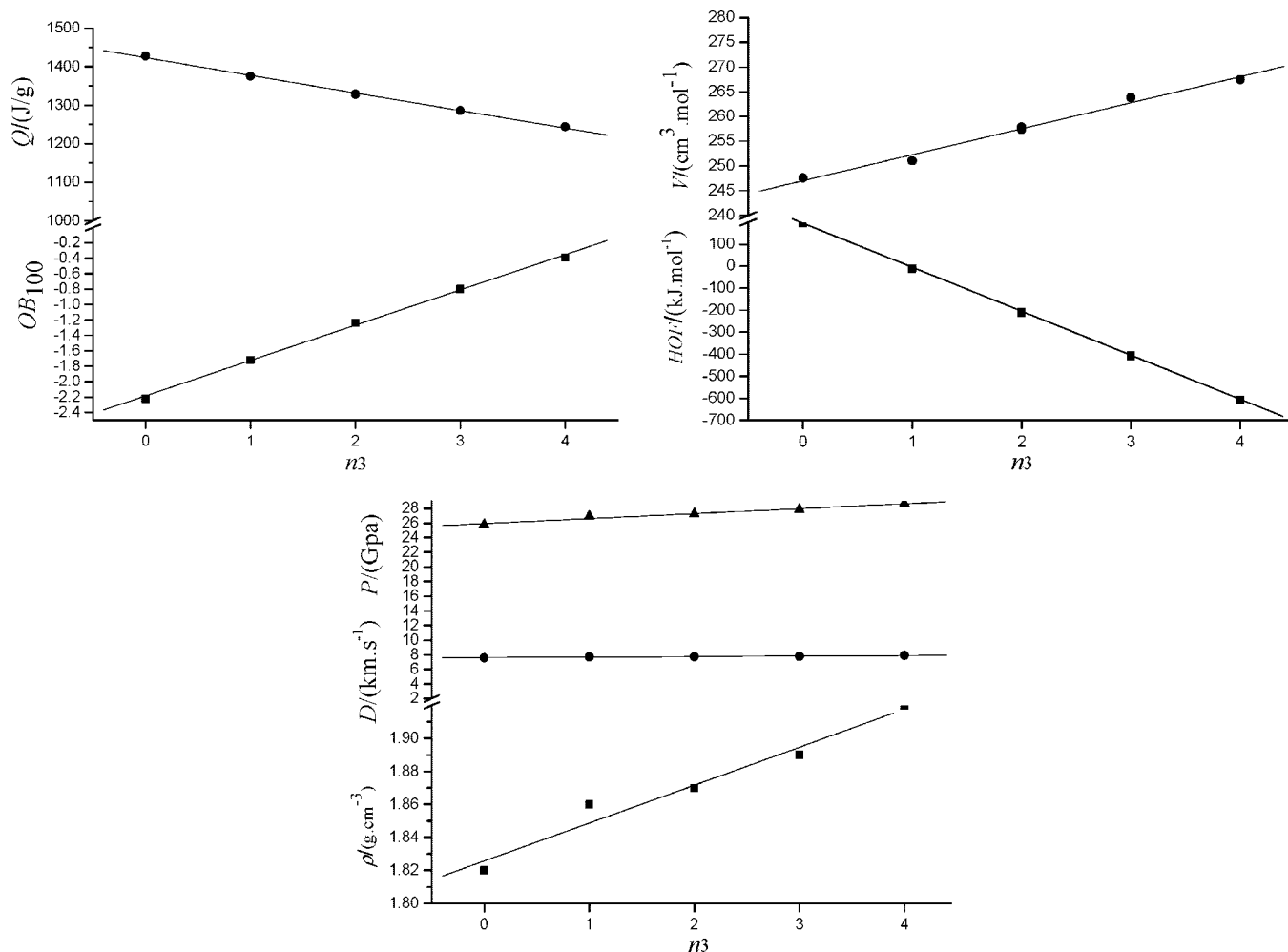


Figure 4. Correlations between OB_{100} , ΔH_f , Q , V , ρ , D , P , and the number of hydroxy groups (n_3) for the hydroxy derivatives of HNS.

TABLE 3: Mulliken Bond Populations for the Title Compounds

no.	M_{C-NO_2}	M_{C-C}	M_{C-H}	M_{C-OH}	M_{O-H}	M_{C-NH_2}	M_{N-H}
I-1	0.1468	0.3764	0.3392				
I-2	0.1360	0.3652	0.3388				
I-3	0.1341	0.3601	0.3594				
I-4	0.1251	0.3611	0.3477				
I-5	0.1254	0.3523	0.3509				
I-6	0.1250	0.3660	0.3435				
II-1	0.1468	0.3540	0.3584			0.3544	0.2732
II-2	0.1474	0.3541	0.3589			0.3536	0.2731
II-3	0.1471	0.3606	0.3584			0.3838	0.2668
II-4	0.1494	0.3558	0.3589			0.3512	0.2668
II-5	0.1558	0.3628	0.3633			0.3746	0.2659
III-1	0.1306	0.3590	0.3589	0.3715	0.2127		
III-2	0.1303	0.3606	0.3540	0.3734	0.2125		
III-3	0.1422	0.3552	0.3440	0.3680	0.2184		
III-4	0.1304	0.3567	0.3441	0.3679	0.2127		
III-5	0.1420	0.3618	0.3147	0.3679	0.2142		

recommended if we want to synthesize hydroxy derivatives with good stability.

In a word, comparison of bond overlap populations could primarily be used to identify the pyrolysis mechanism, the stability, and the relative magnitude of the sensitivity of the homologic energetic materials.

3.2.2. Kinetic Parameter. Another main concern for the energetic materials is whether they are kinetically stable enough to be of practical interest. Thus, studies on the bond dissociation or pyrolysis mechanism are important and essential for understanding the decomposition process of the energetic materials

because they are directly relevant to the sensitivity and stability of the energetic compounds. In this paper, seven possible initial steps in the pyrolysis route are considered for the title compounds by breaking the following bonds according to previous studies:³⁷⁻⁴³ (1) C-NO₂; (2) C-C (=C); (3) C-NH₂; (4) N-H; (5) C-OH; (6) O-H, and (7) hydrogen-transfer isomerization reactions of the O-H bond. In all of these studies, the weakest C-NO₂, C-C, C-NH₂, N-H, C-O, and O-H bonds are selected as the breaking bonds based on the Mulliken bonding population analyses at the B3LYP/6-31G* level. It is worth mentioning that at the B3LYP/6-31G* level we failed to

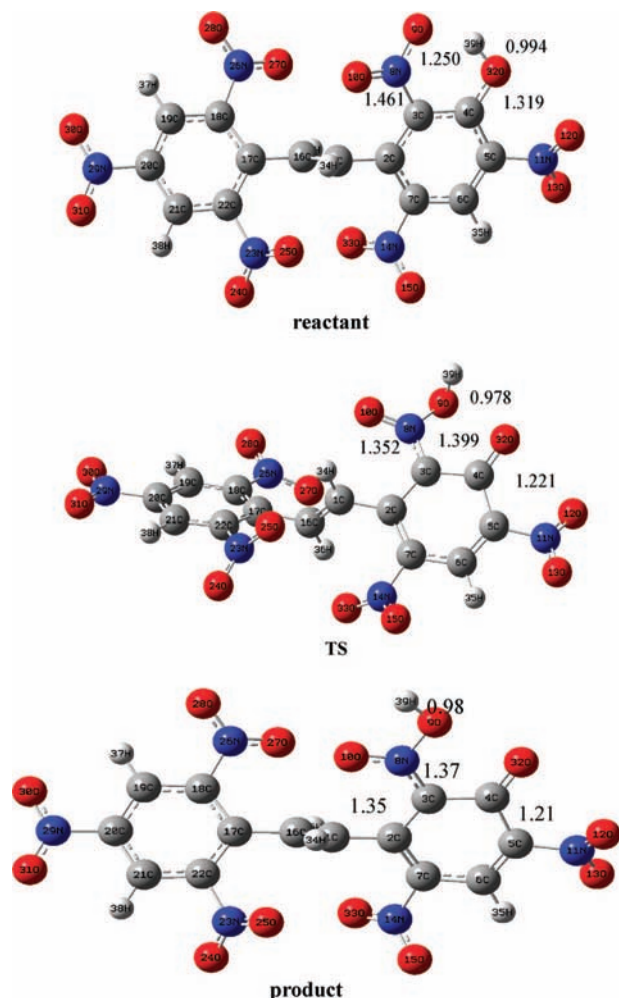


Figure 5. Structures of the reactant, TS, and product fully optimized for the hydrogen-shift isomerization reaction of III-1 and the part of the related geometric parameters.

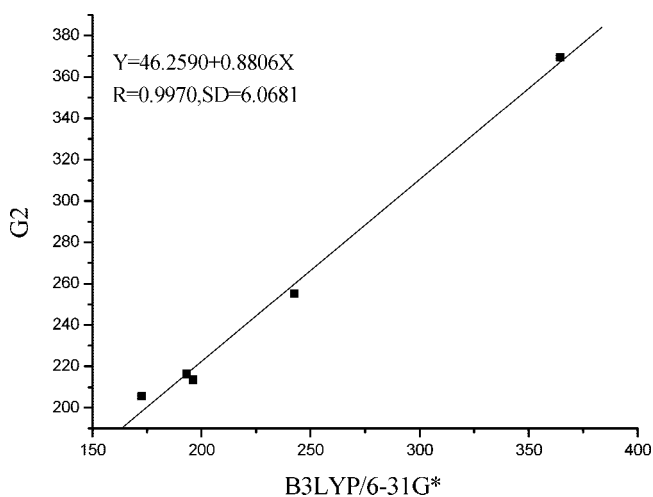


Figure 6. Comparison of the BDEs calculated by the B3LYP/6-31G* and G2 theory.

locate the in-plane transition states (TSs) of the hydrogen shift reactions, but rather we determined the out-of plane TSs, which correspond to the rotation of the O(9)–H(39) bond around the N(8)–O(9) bond (see Figure 5). Interestingly, the in-plane TSs that correspond to the hydrogen shift from O(32) to O(9) can be easily attained at the PM3 level. For comparison, we list the calculated activation energies for both the out-of-plane TSs at

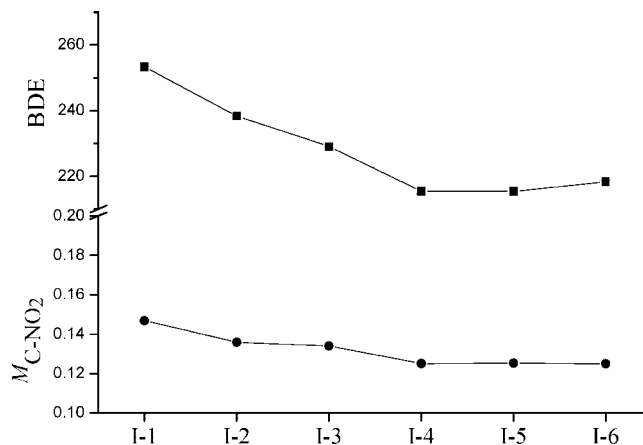


Figure 7. Correlations between BDE, M_{C-NO_2} , and the structures (I-1–I-6).

the B3LYP/6-31G* level and the in-plane TSs at the PM3 level in Table 5. Figure 5 illustrates the structures of the reactant, TS, and product of hydrogen-transfer isomerization reactions fully optimized at the DFT-B3LYP/6-31G* level, including the part of the geometric parameters related with the reaction. The full geometric parameters of the reactant, TS, and product are listed in Tables 1S–3S of the Supporting Information.

First, a benchmark calculation on several small molecules with C–C, C–N, and N–N bonds by using *Gaussian2* (G2) theory⁴⁴ was carried out to check the accuracy of BDE computed with the B3LYP/6-31G* method. Table 4 summarizes the computed BDE values at the G2 and B3LYP/6-31G* levels. Figure 6 shows a very good linear relationship between the B3LYP/6-31G*- and G2-calculated BDEs ($R = 0.9970$). On this basis, we might expect reliable calculated results for the title compounds.

The BDEs and activation energies for the isomerization reactions of the hydrogen transfer (E_a) for the title compounds at the B3LYP/6-31G* level are listed in Table 5. Compared with BDE⁰, BDE parallelly descends 5.6–38.4 kJ/mol, which indicates that using BDEs with or without correction for zero-point energy will not have any influence on the identification of the trigger linkage and pyrolysis mechanism.

Generally speaking, the less energy that is required to break a bond, the weaker the bond is, and the easier the bond becomes a trigger bond; that is to say, the corresponding compound is more unstable, and the sensitivity is larger. From Table 5, it can be seen that, for the nitro and amino derivatives of HNS, BDE of the homolysis of the C–NO₂ bond is the least, which suggests that the C–NO₂ bond may be a trigger bond during the thermolysis initiation process. This validates the conclusion drawn from the above Mulliken population analysis. For the hydroxy derivatives of HNS, E_a of the hydrogen-transfer reaction is much smaller than the BDEs of all bonds, and this illustrates that the homolysis is initiated from breaking of the O–H bond followed by isomerization reactions of the hydrogen transfer, which excludes the possibility of the C–NO₂ bond becoming a trigger bond. At the same time, BDEs of trigger bonds for the title compounds are relatively larger and suffice the stability request of BDE ≈ 80 –120 kJ/mol suggested previously.

In addition, for the nitro derivatives of HNS, with the number of nitro groups increasing, BDE for the homolysis of C–NO₂ bonds decreases, indicating that the stability decreases and their sensitivities increase accordingly. According to the BDEs of a trigger bond (C–NO₂), the order of the stability from I-1 to I-6 is I-6 \approx I-5 \approx I-4 < I-3 < I-2 < I-1. This agrees with the order

TABLE 4: Comparison of Theoretical BDEs (kJ/mol) for Typical C–C, C–N, and N–N Bonds at the G2 and B3LYP/6-31G* Levels

compound	CH ₃ –CH ₃	CH ₃ –NO ₂	NH ₂ –NO ₂	(CH ₃) ₂ N–NO ₂	CH ₃ NH–NO ₂ ^b
B3LYP/6-31G*	364.39	242.55	196.14 (196.65) ^a	172.49	193.07
G2	369.45	255.22	213.72 (213.80) ^b	205.64	216.31

^a Reference 45. ^b Reference 46.

TABLE 5: BDEs for the Main Kinds of Bonds and the Activation Energies of the Hydrogen Transfer in the O–H Bond (kJ/mol)^a

no.	BDE ⁰ /B3LYP/6-31G*							<i>E_a</i> ⁰ /PM3 hydrogentransfer	BDE/B3LYP/6-31G*							<i>E_a</i> /PM3 hydrogentransfer	
	C–NO ₂	C–C	C–NH ₂	N–H	C–O	O–H	O–H ^b		C–NO ₂	C–C	C–NH ₂	N–H	C–O	O–H	O–H ^b		
I-1	269.77	463.51						253.30	444.32								
I-2	255.11	473.26						238.27	453.94								
I-3	244.57	474.39						229.07	455.24								
I-4	231.38	454.82						215.42	436.09								
I-5	231.38	471.87						215.33	471.87								
I-6	234.02	466.58						218.32	446.92								
II-1	255.11	443.86	499.13	447.34				238.31	425.54	468.34	410.00						
II-2	252.47	444.74	493.84	432.45				235.52	426.68	463.09	394.04						
II-3	289.37	442.26	488.59	468.43				272.47	423.57	457.63	430.08						
II-4	249.82	437.85	496.48	468.43				232.76	419.92	466.37	430.46						
II-5	254.31	429.16	490.43	455.60				237.09	410.93	460.19	420.67						
III-1	276.19	445.45			491.53	423.61	123.86	111.59	260.11	426.85			466.83	385.94	117.85		92.66
III-2	276.19	470.06			509.96	425.97	131.80	117.06	260.19	451.54			485.06	387.57	125.12		98.12
III-3	265.40	454.57			496.52	439.42	136.79	127.00	249.31	434.95			472.37	401.31	131.00		106.48
III-4	273.55	441.04			488.88	418.32	134.40	136.56	257.42	421.55			464.90	379.93	128.81		116.64
III-5	263.00	450.91			420.97	420.97	134.40	126.00	247.93	430.21			382.96	382.96	128.60		105.50

^a $E_a = E_{TS} - E_R$, where E_a^0 denotes the activation energies for the isomerization reactions of the hydrogen transfer without zero-point-energy corrections while E_a denotes the activation energies including zero-point-energy corrections; ^b The activation energies of the hydrogen transfer in the O–H bond at the B3LYP/6-31G* level.

deduced from “PSBO” (the principle of the smallest bond orders; i.e., for the series of the energetic materials with the similar molecular structure and pyrolysis mechanism, the smaller the overlap population of the trigger bond, the larger the impact of sensitivity). Figure 7 presents the correlations between BDE, M_{C-NO_2} , and the structures of the nitro derivatives of HNS. The calculated BDEs of breaking of the trigger C–NO₂ bond of the amino derivatives give a stability sequence of II-4 < II-2 < II-5 < II-1 < II-16, which is inconsistent with the ordering derived from the computed bond overlap populations. Such a discrepancy is likely related to the intramolecular hydrogen bonds that are more in the amino derivatives. Because BDE measures the feasibility of a chemical reaction appropriately, we will use it to identify the stability for this series of compounds. For the hydroxy derivatives of HNS, with the number of hydroxy groups increasing, E_a for the isomerization reactions of the hydrogen transfer changes a little but is smaller than the BDE of the C–NO₂ bond for HNS, which indicates that, on the whole, the hydroxy derivatives of HNS are more active than HNS.

In a word, for the derivatives of HNS, bond overlap populations and BDE can be used not only to identify the trigger bond and illustrate the pyrolysis mechanism but also to identify the stability and relative magnitude of the sensitivity.

4. Conclusions

Using the B3LYP/6-31G* method, we have theoretically studied the structures and performance of the derivatives of HNS, and the conclusions of this work are as follows:

(1) For the nitro derivatives of HNS, the oxygen balance, HOF, heat of detonation, volume, density, detonation velocity, and detonation pressure linearly increase with an increase in the number of nitro groups, while for the amino and hydroxy derivatives of HNS, the heat of detonation and HOF linearly decrease with the number of amino and hydroxy groups.

(2) Referring to the bond overlap populations, the homolysis is initiated from breaking of the trigger linkage C–NO₂ bond for the nitro and amino derivatives of HNS, while for the hydroxy derivatives, it is started from breaking of the O–H bond followed by the isomerization reaction of hydrogen transfer.

(3) 2,2',3,3',4,4',5,6,6'-Nonanitrostilbene and 2,2',3,3',4,4',5,5',6,6'-decanitrostilbene essentially satisfy the quantitative criteria of energetics and stability as HEDCs.

(4) The energy and density of HNS are improved when it is substituted with a –NO₂ group, and the insensitivity and stability of HNS are increased by substitution of a –NH₂ group.

Acknowledgment. We gratefully thank the National Natural Science Foundation of China (Grant 10576016), Key Foundation (Grant 10576030), and the National “973” Project for support of this work.

Supporting Information Available: Tables of geometric parameters of the reactant, TS, and product. This material is available free of charge via the Internet at <http://pubs.acs.org>.

References and Notes

- (1) (a) Ship, K. G. *J. Org. Chem.* **1964**, 29, 2620. (b) Ship, K. G.; Kaplan, L. A. *J. Org. Chem.* **1966**, 31, 857.
- (2) Michael, K.; Dagley, I. J.; Whelan, D. J. *J. Phys. Chem.* **1992**, 96, 8001.
- (3) Lu, M. *Acta Armamentarii* **1994**, 2, 46.
- (4) Lee, J. S.; Hsu, C. K.; Chang, C. L. *Thermochim. Acta* **2002**, 392, 173.
- (5) Chen, Z. Q.; Zheng, X. H.; Liu, Z. R.; Pan, Q.; Wang, Y. *Chin. J. Energ. Mater.* **2005**, 13, 249.
- (6) Zhou, J. H.; Chi, Y.; Wang, X. F.; Li, J. S.; Shen, Y. X. *Chin. J. Explos. Propellants* **2006**, 29, 38–40.
- (7) Xiao, H. M. *The Molecular Orbital Theory of Nitro Compounds*; National Defence Industry Press: Beijing, 1993.
- (8) Zhang, J.; Xiao, H. M. *J. Chem. Phys.* **2002**, 116, 10674.

- (9) Xu, X. J.; Xiao, H. M.; Gong, X. D.; Ju, X. H.; Chen, Z. X. *J. Phys. Chem. A* **2005**, *109*, 11268.
- (10) Xu, X. J.; Xiao, H. M.; Ju, X. H.; Gong, X. D.; Zhu, W. H. *J. Phys. Chem. A* **2006**, *110*, 5929.
- (11) Qiu, L.; Xiao, H. M.; Gong, X. D.; Ju, X. H.; Zhu, W. H. *J. Phys. Chem. A* **2006**, *110*, 3797.
- (12) Qiu, L.; Xiao, H. M.; Ju, X. H.; Gong, X. D. *Int. J. Quantum Chem.* **2005**, *105*, 48.
- (13) Qiu, L.; Xiao, H. M.; Gong, X. D.; Ju, X. H. *Chin. J. Struct. Chem.* **2006**, *25*, 1309.
- (14) Xu, X. J.; Xiao, H. M.; Ma, X. F.; Ju, X. H. *Int. J. Quantum Chem.* **2006**, *106*, 1561.
- (15) Xu, X. J.; Xiao, H. M.; Wang, G. X.; Ju, X. H. *Chin. J. Chem. Phys.* **2006**, *19*, 395.
- (16) Xiao, H. M.; Zhang, J. *Sci. China, Ser. B* **2002**, *45*, 21.
- (17) Xiao, H. M.; Xu, X. J.; Qiu, L. *Theoretical Design of High Energy Density Materials*; Science Press: Beijing, 2008.
- (18) Wang, Z. Y. *Aviat. Missile* **2003**, *2*, 34.
- (19) Chen, Z. X.; Xiao, J. M.; Xiao, H. M.; Chiu, Y. N. *J. Phys. Chem. A* **1999**, *103*, 8062.
- (20) Lee, C.; Yang, W.; Parr, R. G. *Phys. Rev. B* **1988**, *37*, 785.
- (21) Becke, A. D. *J. Chem. Phys.* **1992**, *97*, 9173.
- (22) Hariharan, P. C.; Pople, J. A. *Theor. Chim. Acta* **1973**, *28*, 213.
- (23) Frisch, M. J.; Trucks, G. W.; Schlegel, H. B.; Scuseria, G. E.; Robb, M. A.; Cheeseman, J. R.; Montgomery, J. A.; Vreven, J. T.; Kudin, K. N.; Burant, J. C.; Millam, J. M.; Iyengar, S. S.; Tomasi, J.; Barone, V.; Mennucci, B.; Cossi, M.; Scalmani, G.; Rega, N.; Petersson, G. A.; Nakatsuji, H.; Hada, M.; Ehara, M.; Toyota, K.; Fukuda, R.; Hasegawa, J.; Ishida, M.; Nakajima, T.; Honda, Y.; Kitao, O.; Nakai, H.; Klene, M.; Li, X.; Knox, J. E.; Hratchian, H. P.; Cross, J. B.; Adamo, C.; Jaramillo, J.; Gomperts, R.; Stratmann, R. E.; Yazyev, O.; Austin, A. J.; Cammi, R.; Pomelli, C.; Ochterski, J. W.; Ayala, P. Y.; Morokuma, K.; Voth, G. A.; Salvador, P.; Dannenberg, J. J.; Zakrzewski, V. G.; Dapprich, S.; Daniels, A. D.; Strain, M. C.; Farkas, O.; Malick, D. K.; Rabuck, A. D.; Raghavachari, K.; Foresman, J. B.; Ortiz, J. V.; Cui, Q.; Baboul, A. G.; Clifford, S.; Cioslowski, J.; Stefanov, B. B.; Liu, G.; Liashenko, A.; Piskorz, P.; Komaromi, I.; Martin, R. L.; Fox, D. J.; Keith, T.; Al-Laham, M. A.; Peng, C. Y.; Nanayakkara, A.; Challacombe, M.; Gill, P. M. W.; Johnson, B.; Chen, W.; Wong, M. W.; Gonzalez, C.; Pople, J. A. *Gaussian 03*; Gaussian, Inc.: Pittsburgh, PA, 2003.
- (24) Kamlet, M. J.; Jacobs, S. J. *J. Chem. Phys.* **1968**, *48*, 23.
- (25) Zhang, X. H.; Yun, Z. H. *Explosive Chemistry*; National Defence Industry Press: Beijing, 1989.
- (26) Stewart, J. J. P. *J. Comput. Chem.* **1989**, *10*, 209.
- (27) (a) Goh, E. M.; Cho, S. G.; Park, B. S. *J. Def. Technol. Res.* **2000**, *6*, 91. (b) Dorsett, H.; White, A. Aeronautical and Maritime Research Laboratory, Defence Science & Technology Organization (DSTO). DSTO Technical Report DSTO-GD-0253, Australia, **2000**. (c) Sikder, A. K.; Maddala, G.; Agrawal, J. P.; Singh, H. *J. Hazard. Mater. A* **2001**, *84*, 1.
- (28) Stine, J. R. Los Alamos National Laboratory's Report, Los Alamos, NM, 1981.
- (29) Ammon, H. L. *Struct. Chem.* **2001**, *12*, 205.
- (30) Karfunkel, H. R.; Gdanitz, R. J. *J. Comput. Chem.* **1992**, *13*, 1171.
- (31) Rice, B. M.; Sorescu, D. C. *J. Phys. Chem. B* **2004**, *108*, 17730.
- (32) Qiu, L.; Xiao, H. M.; Gong, X. D.; Ju, X. H.; Zhu, W. *J. Hazard. Mater.* **2007**, *141*, 280.
- (33) Lide, D. R., Ed. *CRC Handbook of Chemistry and Physics*; CRC Press LLC: Boca Raton, FL, 2002.
- (34) Kamlet, M. J.; Adolph, H. G. *Propellants, Explos., Pyrotech.* **1979**, *4*, 30.
- (35) Dong, H. S.; Zhou, F. F. *High energy explosives and their corresponding performance*; Science Press: Beijing, 1989.
- (36) Mulliken, R. S. *J. Chem. Phys.* **1955**, *23*, 1833.
- (37) Manelis, G. B.; Nazin, G. M.; Rubtsov, Yu. I.; Strunin, V. A. *Combustion of Explosives and Powders*; Taylor & Francis Group: Oxford, U.K., 2003.
- (38) Turovec, A. G.; Danilova, V. I. *Izv. Vyssh. Uchebn. Zaved., Fiz.* **1973**, *8*, 68.
- (39) Bulusu, S.; Axenrod, T. *Org. Mass Spectrom.* **1979**, *14*, 585.
- (40) Wang, J.; Lang, H. Y. *Sci. China, Ser. B* **1990**, *33*, 257.
- (41) Varga, R.; Zeman, S. *J. Hazard. Mater. A* **2006**, *132*, 165.
- (42) Varga, R.; Zeman, S.; Kouba, M. *J. Hazard. Mater. A* **2006**, *132*, 1345.
- (43) Bulusu, S.; Autera, J. R. *J. Energ. Mater.* **1983**, *1*, 133.
- (44) Curtiss, L. A.; Carpenter, J. E.; Raghavachari, K.; Pople, J. A. *J. Chem. Phys.* **1991**, *94*, 7221.
- (45) Politzer, P.; Lane, P. *J. Mol. Struct. (Theochem)* **1996**, *388*, 51.
- (46) Harris, N. J.; Lammertsma, K. *J. Am. Chem. Soc.* **1997**, *119*, 6583.